Electronic Transitions of Ternary Copper(II) Naphthalenediolate Complexes

Yasunori Yamada,# Miki Hasegawa, Michio Kobayashi, Yutaka Fukuda,† and Toshihiko Hoshi*

Department of Chemistry, College of Science and Engineering, Aoyama Gakuin University, 6-16-1 Chitosedai, Setagaya-ku, Tokyo 156

†Department of Chemistry, Faculty of Science, Ochanomizu University, 2-1-1 Otsuka, Bunkyo-ku, Tokyo 112

(Received July 3, 1997)

The electronic structure and nature of the electronic transitions of copper(II) naphthalenediolate complexes, (2, 2′-bipyridine) (2,3-naphthalenediolato) copper(II) ([Cu(ndo)(bpy)]) and (2,3-naphthalenediolato) (1,10-phenanthroline) copper(II) ([Cu(ndo)(phen)]), have been studied from the viewpoints of the polarization spectra and MO theory. The 339.0 and 296 nm bands of [Cu(ndo)(phen)] have been assigned to localized transitions of the naphthalenediolate (ndo) skeleton, and the 308, 275, and 269 nm bands on the phenanthroline (phen) skeleton. It has been clarified experimentally that the 400 nm band can be assigned to the CT transition between ndo and Cu(II). The total state wavefunctions show that the 293 and 282 nm bands are due to the intramolecular interligand CT (LL′CT) transitions from ndo to phen, thus indicating that the two π-electronic systems, separated by the central metal ion, can directly interact. The complex [Cu(ndo)(bpy)] shows the electronic transitions at 339.0, 256.0, 245, 238, and 210 nm localized on ndo, and at 315, 295, and 264 nm localized on the bipyridine (bpy) moiety. The 400 nm band of [Cu(ndo)(bpy)] is due to the intramolecular CT transition between ndo and Cu(II). In the case of [Cu(ndo)(bpy)], the LL′CT transition is not observed.

It is well known that diimine-type ligands, such as 2, 2′-bipyridine (bpy) and 1,10-phenanthroline (phen), form very stable ternary copper(II) complexes with catecholate (cat).[1—3] Sigel et al. considered that the high stabilities of the above-mentioned complexes are based on interactions between two kinds of ligands.[1] However, they give no experimental or theoretical evidence for the existence of this interaction. Recently, evidence concerning interligand interactions has been shown from the viewpoints of spectroscopy and quantum-mechanical calculations.[4,5] In the case of (catecholato)(1,10-phenanthroline)copper(II) ([Cu(cat)(phen)]), for instance, two π-electronic systems of the two ligands, cat and phen, are significantly mixed through configuration interactions.[4]

In the spectrum of (2,2′-bipyridine)(catecholato)copper(II) ([Cu(cat)(bpy)]), a $\pi\pi^*$ interligand charge-transfer (LL′CT) band from cat to bpy has been found.[5] This indicates that two π-electronic systems of the two ligands interact directly, in which the π-electronic system of cat acts as an electron donor, and the system of bpy or phen acts as an electron acceptor. In order to understand the nature of the mechanism of interligand electronic interactions in more detail, it is important to accumulate experimental data concerning the electronic transitions of ternary complexes. Brown et al. measured the electronic spectra of (2, 2′-bipyridine)(2,3-naphthalenediolato)copper(II) ([Cu(ndo)(bpy)]) and (2,3-naphthalenediolato)(1,10-phenanthroline)copper(II) ([Cu(ndo)(phen)]) in dimethylsulfoxide, but did not give detailed interpretations.[6] In the present investigation, the polarized absorption spectra of [Cu(ndo)(bpy)] and [Cu(ndo)(phen)] were measured in stretched poly(vinyl alcohol) (PVA) film, and the polarization of each electronic transition was determined. The electronic spectra of the above two complexes were compared with those of (2, 2′-bipyridine)(oxalato)copper(II) ([Cu(ox)(bpy)]), (oxalato)-(1,10-phenanthroline)copper(II) ([Cu(ndo)(phen)]) and (ethylenediamine)(2,3-naphthalenediolato)copper(II) ([Cu(ndo)-(en)]). Also, the origins and nature of the electronic transitions have been elucidated in conjunction with the results of MO calculations due to a modified PPP method.[4,5,7]

Experimental and MO Calculations

The complexes [Cu(ndo)(bpy)], [Cu(ndo)(phen)], [Cu(ndo)-(en)], and [Cu(ox)(bpy)] were synthesized and purified by an already described method.[6,8] Methanol, used to measure the electronic absorption spectra, was distilled. Stretched PVA films containing sample molecules were prepared by a previously described method.[9—11] A Shimadzu UV3101-PC spectrophotometer was used to measure the electronic absorption spectra. Polarized absorption spectra were measured with the above-mentioned spectrophotometer equipped with a Rochon-type polarizer.

A modified PPP method, which can be applied to calculate π-electronic systems of metal complexes, was used.[4,5,7,12] The bond lengths and angles used for the present MO calculation were taken from the literature[13—17] concerning X-ray diffraction analyses for [Cu(ox)(bpy)] and [Cu(ox)(phen)]. That is, the following inter-

Present address: Department of Chemistry, University of Tsukuba, Tennodai 1-1-1, Tsukuba, Ibaraki 305.

atomic bond lengths and angles were used: Cu–O$^-$ = 1.95, Cu–N = 1.95, C–C = 1.395, C–N = 1.395 Å, ∠NCuN = 88, ∠O$^-$CuO$^-$ = 87°. The bond angle ∠O$^-$CuO$^-$ is assumed in analogy with the result of an X-ray analysis concerning [Cu(ox)(bpy)].

Results and Discussion

(2,2′-Bipyridine)(oxalato)copper(II). The absorption spectrum of [Cu(ox)(bpy)] measured in a 1 : 1 mixed solvent of methanol and water (abbreviated to aq MeOH) is shown in Fig. 1a. The [Cu(ox)(bpy)] complex shows absorption bands at 625, 310.5, 300.0, 290, 258, 250, and 211 nm. It is evident, from the intensity and location that the 625 nm band is due to a d–d transition. Figure 1b shows the polarized absorption spectrum of [Cu(ox)(bpy)] in stretched PVA film. In this figure, $D_{\parallel}$ and $D_{\perp}$ are the optical densities measured with light beams polarized parallel and perpendicular to the stretch direction of the PVA film, respectively and $R_d = D_{\parallel}/D_{\perp}$. R_s is the stretch ratio of the PVA film. The 310.5, 300.0, 290, 258, 250, and 211 nm bands measured in aq MeOH appear

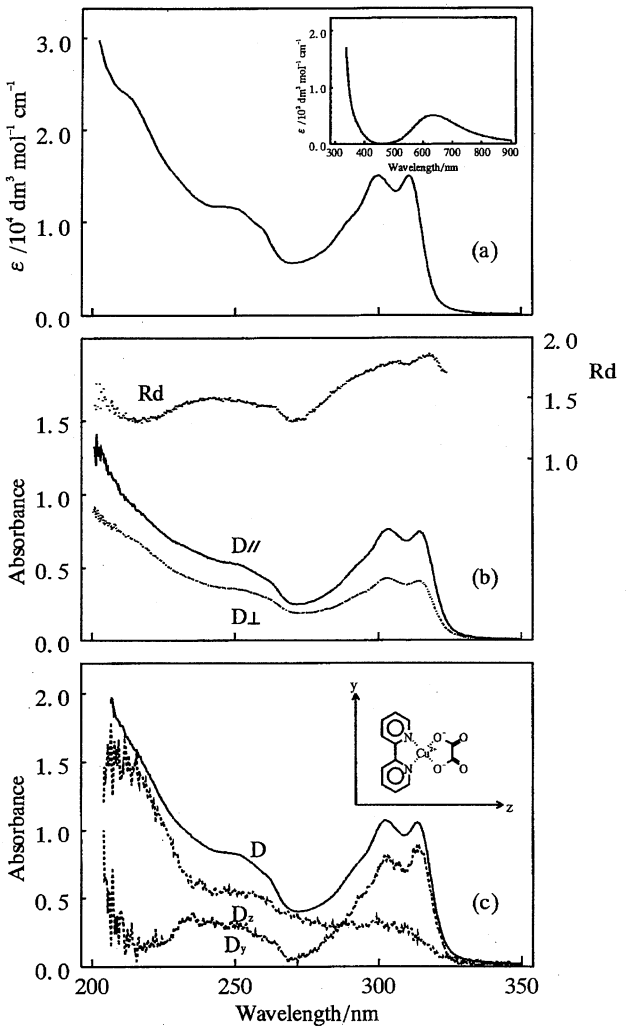

Fig. 1. The electronic absorption, polarized absorption, and reduced spectra of [Cu(ox)(bpy)]; (a) the absorption spectrum in aq MeOH; (b) the polarized absorption spectrum in the stretched PVA film (R_s = 8.8); (c) the reduced spectra in the PVA film.

at 314.5, 304.0, 294, 260, 252, and 211 nm in the stretched PVA film, respectively. Generally, the long axes of the guest molecules are inclined preferentially to the stretch direction of the PVA film.[9,10] However, in the case of the [Cu(ox)(bpy)] molecule, the shape of the molecule is almost square planar. A comparison of the polarization spectrum and MO calculation described later shows that the axis (*y*-axis) perpendicular to the C_2-axis orients preferentially to the stretch direction of the PVA film. This means that the electronic band with large R_d values is polarized along the *y*-axis, and the band with small values along the *z* (C_2) axis. The 314.5 nm band with large R_d values and the 211 nm band with small R_d values are polarized along the *y*- and *z*-axes, respectively. Based on the polarization spectrum using stretched PVA film, in order to know the polarization direction of the other bands, the absorption spectrum (D) of [Cu(ox)(bpy)] in the isotropic PVA film was deconvoluted into two reduced spectra polarized along the *y*- (D_y) and *z*-axes (D_z) (Fig. 1c). As can be seen from this figure, [Cu(ox)(bpy)] shows the *y*-axis polarized electronic bands at 314.5, 304.0, 294, 260, and 235 nm, and the *z*-axis polarized ones at 295, 252, 225, and 211 nm. The 304.0 and 294 nm bands are considered to be vibronic bands originating at 314.5 nm, whose progression is 1100 cm^{-1}. For the following two reasons, the 252 and 235 nm bands are assigned to the intramolecular (LM or ML) CT transitions between copper(II) and bpy and between copper(II) and oxalate (ox), respectively: (1) The transitions corresponding to the 252 (*z*-axis polarized) and 235 nm (*y*-axis polarized) bands are not seen in the MO calculated result described later. (2) [Cu(cat)(bpy)] shows the corresponding transition to the above 252 nm band at 245 nm, while it shows no corresponding transition to the 235 nm band.[5] The above experimental results are summarized in Table 1 compared with the MO calculation. The *y*-axis polarized 314.5 and 260 nm bands are assigned to the calculated $\pi\pi^*_1$ and $\pi\pi^*_3$ transitions, respectively, and the *z*-axis polarized 295, 225, and 211 nm bands to the $\pi\pi^*_2$, $\pi\pi^*_4$, and $\pi\pi^*_6$ transitions, respectively. The excited-state wavefunctions for these $\pi\pi^*$ transitions are given as follows:

$$\begin{aligned}
\Psi_1 &= -0.8837\,\chi_{10,11} + \cdots \\
\Psi_2 &= -0.5759\,\chi_{9,11} - 0.6834\,\chi_{10,13} + \cdots \\
\Psi_3 &= 0.4148\,\chi_{10,11} - 0.6933\,\chi_{10,14} + \cdots \\
\Psi_4 &= -0.7179\,\chi_{6,11} + 0.3954\,\chi_{9,11} + \cdots \\
\Psi_5 &= 0.5726\,\chi_{8,11} - 0.5594\,\chi_{10,14} + \cdots \\
\Psi_6 &= 0.5818\,\chi_{9,11} + 0.5483\,\chi_{10,15} + \cdots,
\end{aligned} \tag{1}$$

where $\chi_{i,j}$ represents the one-electron excited configuration wavefunction from the *i*'th occupied orbital to the *j*'th vacant orbital (Eq. 1). The diagrammatic representations of the MO's concerned with the above state wavefunctions are shown in Fig. 2. The main contributor to Ψ_1 corresponding to the $\pi\pi^*_1$ transition is $\chi_{10,11}$. Since MO's ϕ_{10} and ϕ_{11} are localized orbitals on the bpy skeleton, the observed 314.5 nm band can be regarded as being due to a localized transition on bpy. Likewise, the 295, 260, 225, and 211 nm bands are

Table 1. Comparison of the Calculated and Observed Results for the Electronic Transitions of [Cu(ox)(bpy)];

		Transition energy (nm)		Intensity		Polarization direction	
		Calcd	Obsd[a)]	Calcd[b)]	Obsd[c)]	Calcd	Obsd[a)]
			625[d),e)]		—		—
$\pi\pi^*_1$	($^1B_1$)	307.1	314.5	0.51553	0.539	*y*	*y*
$\pi\pi^*_2$	($^1A_1$)	280.6	295	0.01864	0.216	*z*	*z*
$\pi\pi^*_3$	($^1B_1$)	254.0	260	0.24768	0.196	*y*	*y*
			252[f)]		0.277		*z*
			235[f)]		0.200		*y*
$\pi\pi^*_4$	($^1A_1$)	224.3	225	0.01853	0.667	*z*	*z*
$\pi\pi^*_5$	($^1B_1$)	212.8		0.01882		*y*	
$\pi\pi^*_6$	($^1A_1$)	212.4	211	0.38670	1.000	*z*	*z*

a) Observed in the PVA matrix at room temperature. *y*: Perpendicular to the C_2 axis in the molecular plane. *z*: The C_2 axis. b) Oscillator strength. c) Relative intensities with respect to the 211 nm band. d) Observed in methanol. e) d–d Band. f) Intramolecular CT band between copper(II) and bpy (or ox).

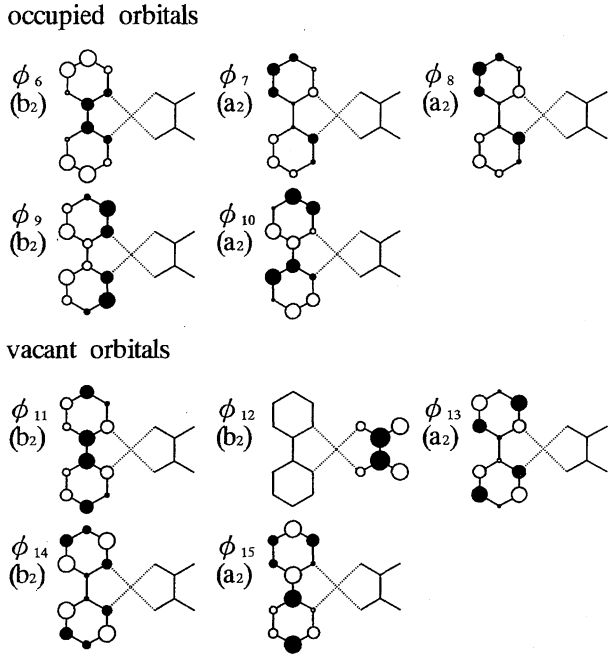

Fig. 2. Diagrammatic representation of SCF MO's of [Cu(ox)(bpy)].

localized transitions on bpy.

(Ethylenediamine)(2,3-naphthalenediolato)copper(II). The complex [Cu(ndo)(en)] shows electronic absorption bands at 625, 400, 338.0, 325, 313, 295, 253, 247.5, and 210 nm in methanol (Fig. 3a). The 625 nm band is evidently due to a d–d transition. The 400 nm band is considered to be assigned as an intramolecular CT transition between Cu(II) and naphthalenediolate (ndo) (or ethylenediamine), because the corresponding transition is not computed out in the MO calculation. Judging from the progression, the 325 and 313 nm bands are vibronic transitions originating at 338.0 nm. The 338.0, 325, 313, 295, 253, 247.0, and 210 nm bands measured in methanol are red-shifted by 0—5 nm in the PVA film, and appear at 340.0, 327, 315, 300, 255.5, 251, and 210 nm, respectively (Fig. 3b). The R_d curve shows a maximum

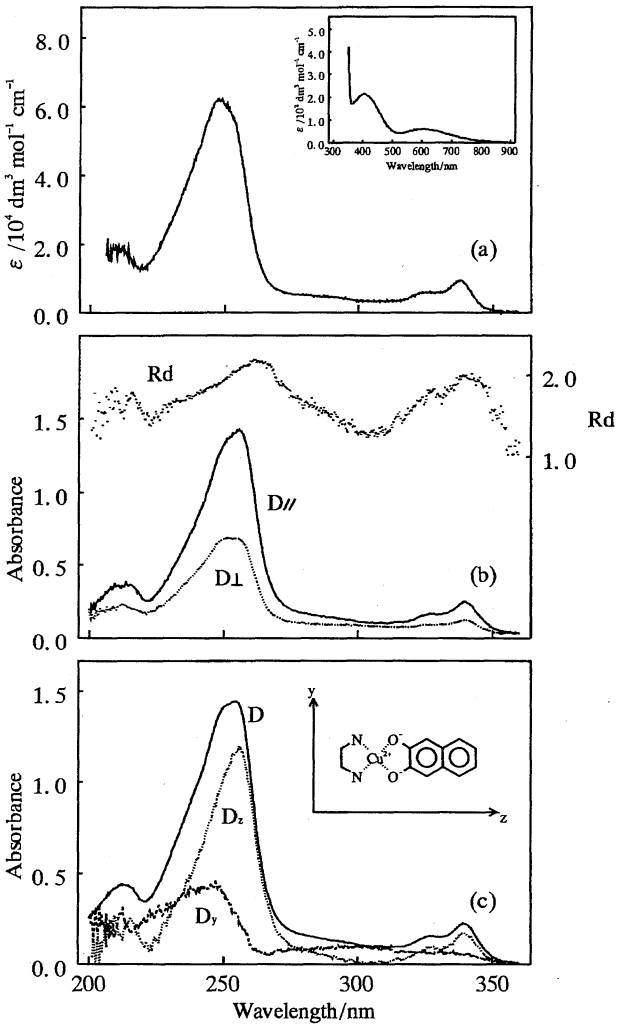

Fig. 3. The electronic absorption, polarized absorption, and reduced spectra of [Cu(ndo)(en)] (a) the absorption spectrum in methanol; (b) the polarized absorption spectrum in the stretched PVA film (R_s=8.3); (c) the reduced spectra in the PVA film.

at around 340 nm and a minimum at around 300 nm, this indicating that the 340 nm band is polarized along the z (C_2) axis, and the 300 nm band along the y-axis (perpendicular to the C_2-axis in the molecular plane). The R_d curve shows a peak at 260 nm, which does not coincide with the location of the intense 255.5 nm band, and is gradually lowered toward the higher energy side. This means that the intense 255.5 nm band is composed of at least two differently polarized electronic transitions. According to the reduced polarization spectrum, it is seen that, in the wavelength region 200—260 nm, the z-axis polarized electronic bands are at 255.5 and 210 nm, and the y-axis polarized bands at 246 and 238 nm (Fig. 3c). The z-axis polarized 340.0 and 210 nm bands are assigned to the calculated $\pi\pi^*_1$ and $\pi\pi^*_8$ transitions, respectively, and the y-axis polarized 300, 246, and 238 nm bands to the $\pi\pi^*_2$, $\pi\pi^*_5$, and $\pi\pi^*_6$ transitions (Table 2). The 255.5 nm band is considered to be an overlap of the $\pi\pi^*_3$ and $\pi\pi^*_4$ transitions. The MO calculation shows that the 340.0, 300, 255.5, 246, 238, and 210 nm bands can be regarded as being localized transitions on the ndo skeleton.

(2, 2′- Bipyridine)(2, 3- naphthalenediolato)copper(II). Figure 4 shows the absorption spectrum measured in methanol (a) and the reduced spectrum in the PVA film (b) of [Cu(ndo)(bpy)]. This compound shows a weak band at 400 nm, and intense bands at 338.0, 310.5, 299.0, and 250 nm in methanol (Fig. 4a). The 338.0 and 299.0 nm bands are accompanied by shoulders at around 325 and 290 nm, respectively. In addition to the above-mentioned bands, [Cu(ndo)(bpy)] shows a weak d–d band at around 650 nm. The transition corresponding to the 400 nm band has been observed in the case of [Cu(ndo)(en)] having the ndo skeleton. However, in the case of [Cu(ox)(bpy)], which has no ndo skeleton, no band has been observed at around 400 nm. Furthermore, 2,3-napthalenediol shows no absorption band at around 400 nm.[18] Thus, it is evident that the 400 nm band of [Cu(ndo)(bpy)] is due to an intramolecular CT transition between Cu(II) and the π-electronic system of the ndo skeleton. The 338.0, 325, 310.5, 299.0, 290, and 250 nm bands of [Cu(ndo)(bpy)] measured in methanol appear at 339.0, 326, 315, 304, 293, and 256.0 nm in unstretched PVA film, respectively (Fig. 4b). Figure 4b shows that the z-axis polarized bands are at 339.0, 295, 256.0, and 210 nm, in which the 295 and 210 nm bands are not found clearly in methanol. The y-polarized bands are at 315, 264, 245, and 238 nm. In addition to the above-mentioned bands, the z-axis polarized bands are found at 326 and 313 nm, and the y-axis polarized ones at 304 and 293 nm. From its progression, the former z-axis polarized bands can be interpreted as being vibronic bands of the 339.0 nm electronic band, and the latter y-axis polarized ones as of the 315 nm electronic band. Judging from the intensi-

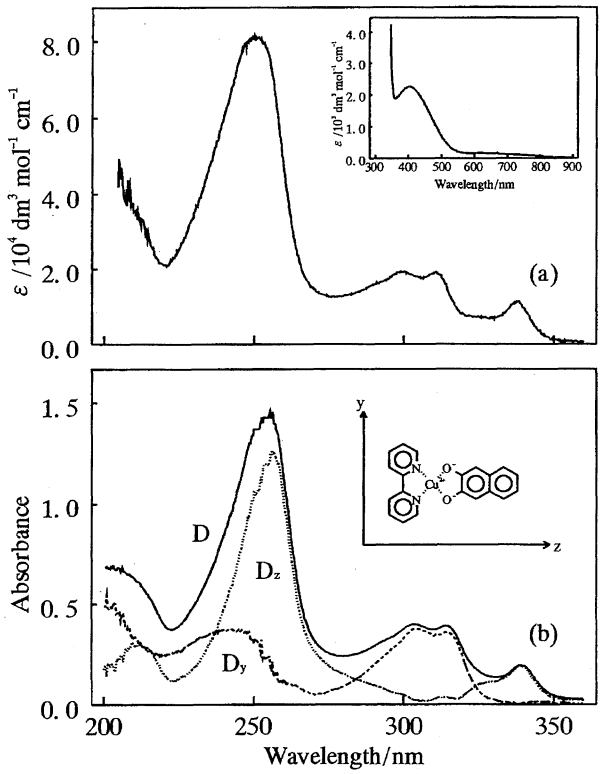

Fig. 4. The electronic absorption and reduced spectra of [Cu(ndo)(bpy)]; (a) the absorption spectrum in methanol; (b) the reduced spectra in the PVA film.

Table 2. Comparison of the Calculated and Observed Results for the Electronic Transitions of [Cu(ndo)(en)]

		Transition energy (nm)		Intensity		Polarization direction	
		Calcd	Obsd[a]	Calcd[b]	Obsd[c]	Calcd	Obsd[a]
			625[d),e)]		—		—
			400[d),f)]		—		—
$\pi\pi^*_1$	($^1A_1$)	347.2	340.0	0.01848	0.041	z	z
$\pi\pi^*_2$	($^1B_1$)	305.5	300	0.11253	0.081	y	y
$\pi\pi^*_3$	($^1A_1$)	252.2	255.5	1.05854	1.000	z	z
$\pi\pi^*_4$	($^1A_1$)	239.4		0.90255		z	
$\pi\pi^*_5$	($^1B_1$)	238.7	246	0.43754	0.374	y	y
$\pi\pi^*_6$	($^1B_1$)	229.8	238	0.15201	0.323	y	y
$\pi\pi^*_7$	($^1B_1$)	220.9		0.00304		y	
$\pi\pi^*_8$	($^1A_1$)	205.2	210	0.04175	0.212	z	z

a) Observed in the PVA matrix at room temperature. y: Perpendicular to the C_2 axis in the molecular plane. z: The C_2 axis. b) Oscillator strength. c) Relative intensities with respect to the 255.5 nm band. d) Observed in methanol. e) d–d Band. f) Intramolecular CT band between copper(II) and ndo (or en).

ties and polarizations, the 339.0, 256.0, 245, 238, and 210 nm bands of [Cu(ndo)(bpy)] correspond to the 340.0 ($\pi\pi^*_1$), 255.5 ($\pi\pi^*_3$), 246 ($\pi\pi^*_5$), 238 ($\pi\pi^*_6$), and 210 nm ($\pi\pi^*_8$) bands in [Cu(ndo)(en)], and the 315, 293, and 264 nm bands to the 314.5 ($\pi\pi^*_1$), 295 ($\pi\pi^*_2$), and 260 nm ($\pi\pi^*_3$) bands in [Cu(ox)(bpy)], respectively. The above experimental results have been compared with the calculated ones given in Table 3. The z-axis polarized 339.0, 295, 256.0, and 210 nm bands are assigned to the $\pi\pi^*_1$, $\pi\pi^*_6$, $\pi\pi^*_{10}$, and $\pi\pi^*_{23}$ transitions, and the y-axis polarized 315, 264, 245, and 238 nm bands to the $\pi\pi^*_2$, $\pi\pi^*_7$, $\pi\pi^*_{13}$, and $\pi\pi^*_{15}$ transitions, respectively. According to the excited-state wavefunctions (Eq. 2), $\chi_{12,17}$ and $\chi_{13,19}$ contribute to Ψ_1 corresponding to the $\pi\pi^*_1$ transition by 60 and 37%, respectively.

$$\Psi_1 = -0.7778\,\chi_{12,17} + 0.6106\,\chi_{13,19} + \cdots$$
$$\Psi_2 = -0.8711\,\chi_{11,14} + \cdots$$
$$\Psi_3 = 0.8150\,\chi_{13,14} - 0.5219\,\chi_{13,17} + \cdots$$
$$\Psi_4 = 0.9743\,\chi_{12,14} + \cdots$$
$$\Psi_5 = 0.5525\,\chi_{13,14} + 0.7695\,\chi_{13,17} + \cdots$$
$$\Psi_6 = -0.5731\,\chi_{8,14} + 0.6824\,\chi_{11,15} + \cdots$$
$$\Psi_7 = -0.4653\,\chi_{7,14} - 0.6870\,\chi_{11,16} + \cdots$$
$$\Psi_8 = -0.9112\,\chi_{13,15} + \cdots$$
$$\Psi_9 = -0.8515\,\chi_{12,15} - 0.4769\,\chi_{13,16} + \cdots$$
$$\Psi_{10} = -0.5600\,\chi_{12,17} - 0.7140\,\chi_{13,19} + \cdots$$
$$\Psi_{11} = -0.4890\,\chi_{12,15} - 0.8610\,\chi_{13,16} + \cdots \quad (2)$$
$$\Psi_{12} = 0.9072\,\chi_{12,16} + \cdots$$
$$\Psi_{13} = 0.8560\,\chi_{12,19} + \cdots$$
$$\Psi_{14} = -0.5611\,\chi_{10,19} + 0.6462\,\chi_{12,20} + \cdots$$
$$\Psi_{15} = -0.6963\,\chi_{10,17} + 0.6169\,\chi_{13,20} + \cdots$$
$$\Psi_{16} = -0.6976\,\chi_{6,14} + 0.3939\,\chi_{8,14} + \cdots$$
$$\Psi_{17} = -0.6383\,\chi_{10,17} - 0.7600\,\chi_{13,20} + \cdots$$
$$\Psi_{18} = 0.7485\,\chi_{7,14} - 0.5935\,\chi_{11,16} + \cdots$$
$$\Psi_{19} = 0.5859\,\chi_{8,14} - 0.5903\,\chi_{11,18} + \cdots$$
$$\Psi_{20} = 0.9378\,\chi_{10,14} + \cdots$$
$$\Psi_{21} = -0.9810\,\chi_{13,18} + \cdots$$
$$\Psi_{22} = 0.9353\,\chi_{12,18} + \cdots$$
$$\Psi_{23} = 0.8772\,\chi_{9,17} + \cdots$$

Since all the MO's ϕ_{12}, ϕ_{13}, ϕ_{17}, and ϕ_{19} are localized on the ndo skeleton (Fig. 5), the observed 339.0 nm band is regarded as being a localized transition on ndo. Similarly, the 256.0, 245, 238, and 210 nm bands are also due to localized transitions on ndo. On the other hand, the main contributor to Ψ_2 is $\chi_{11,14}$, which corresponds to one-electron excitation from ϕ_{11} to ϕ_{14}, both localized on bpy. Thus, the 315 nm

Table 3. Comparison of the Calculated and Observed Results for the Electronic Transitions of [Cu(ndo)(bpy)]

		Transition energy (nm)		Intensity		Polarization direction	
		Calcd	Obsd[a)]	Calcd[b)]	Obsd[c)]	Calcd	Obsd[a)]
			650[d),e)]		—		—
			400[d),f)]		—		—
$\pi\pi^*_1$	($^1A_1$)	341.0	339.0	0.04083	0.156	z	z
$\pi\pi^*_2$	($^1B_1$)	305.7	315	0.41803	0.283	y	y
$\pi\pi^*_3$	($^1B_1$)	303.4		0.04612		y	
$\pi\pi^*_4$	($^1A_1$)	302.9		0.00038		z	
$\pi\pi^*_5$	($^1B_1$)	302.8		0.11361		y	
$\pi\pi^*_6$	($^1A_1$)	279.9	295	0.02141	0.049	z	z
$\pi\pi^*_7$	($^1B_1$)	253.3	264	0.22052	0.078	y	y
$\pi\pi^*_8$	($^1A_1$)	252.3		0.00750		z	z
$\pi\pi^*_9$	($^1B_1$)	251.6		0.00050		y	
$\pi\pi^*_{10}$	($^1A_1$)	248.7	256.0	1.80169	1.000	z	z
$\pi\pi^*_{11}$	($^1B_1$)	242.6		0.00042		y	
$\pi\pi^*_{12}$	($^1A_1$)	241.4		0.00022		z	
$\pi\pi^*_{13}$	($^1B_1$)	236.8	245	0.48222	0.840	y	y
$\pi\pi^*_{14}$	($^1A_1$)	234.3	(256.0)	0.52231	(0.293)	z	(z)
$\pi\pi^*_{15}$	($^1B_1$)	229.3	238	0.10235	0.264	y	y
$\pi\pi^*_{16}$	($^1A_1$)	221.8		0.00583		z	
$\pi\pi^*_{17}$	($^1B_1$)	220.7		0.00002		y	
$\pi\pi^*_{18}$	($^1B_1$)	211.5		0.03718		y	
$\pi\pi^*_{19}$	($^1A_1$)	210.5		0.10633		z	
$\pi\pi^*_{20}$	($^1B_1$)	207.8		0.00002		y	
$\pi\pi^*_{21}$	($^1A_1$)	207.2		0.00009		z	
$\pi\pi^*_{22}$	($^1B_1$)	205.0		0.00066		y	
$\pi\pi^*_{23}$	($^1A_1$)	203.3	210	0.08925	0.238	z	z

a) Observed in the PVA matrix at room temperature. y: Perpendicular to the C_2 axis in the molecular plane. z: The C_2 axis. b) Oscillator strength. c) Relative intensities with respect to the 256.0 nm band. d) Observed in methanol. e) d–d Band. f) Intramolecular CT band between copper(II) and ndo.

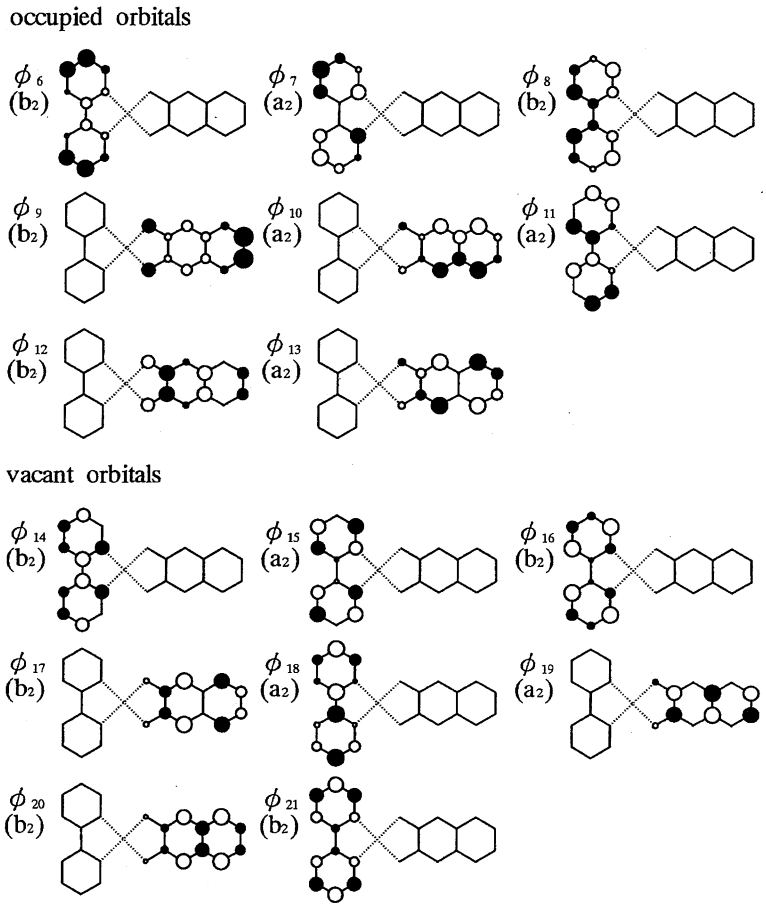

Fig. 5. Diagrammatic representations of SCF MO's of [Cu(ndo)(bpy)].

band of [Cu(ndo)(bpy)] is interpreted as being a localized transition on bpy. Similarly, the 295 and 264 nm transitions are localized on bpy. As described above, the present MO calculation well reproduces the experimental results.

Although the calculated $\pi\pi^*_4$, $\pi\pi^*_8$, and $\pi\pi^*_{12}$ transitions are LL′CT (intramolecular interligand CT) transitions, the corresponding observed bands have not been found. These transitions may be masked by the nearby intense $\pi\pi^*$ bands.

(2,3-Naphthalenediolato)(1,10-phenanthroline)copper-(II). The complex [Cu(ndo)(phen)] shows a d–d band at around 650 nm and an intramolecular CT band between ndo and Cu(II) at 400 nm in methanol (Fig. 6a). In the wavelength region 200—350 nm, this complex shows electronic absorption bands at 337.5, 323, 293, 273, 250.0, 233, and 210 nm; these bands are red-shifted in PVA film, appearing at 339.0, 325, 296, 275, 255.5, 236, and 212 nm, respectively (Fig. 6b). In Fig. 6b, the reduced polarization spectrum of [Cu(ndo)(phen)] is also shown. According to this polarization spectrum, the z-axis polarized bands are at 339.0, 293, 282, 269, 255.5, 236, and 212 nm, and the y-axis polarized ones at 308, 296, 275, 253, and 229 nm. By analogy with the cases of [Cu(ndo)(en)] and [Cu(ndo)(bpy)], the z-axis polarized 325 nm band is due to the vibronic transition of the 339.0 nm electronic band. The z-axis polarized the 339.0, 293, 282, 269, 236, and 212 nm bands are assigned to the $\pi\pi^*_1$, $\pi\pi^*_5$, $\pi\pi^*_7$, $\pi\pi^*_{10}$, $\pi\pi^*_{15}$, and $\pi\pi^*_{26}$ transitions,

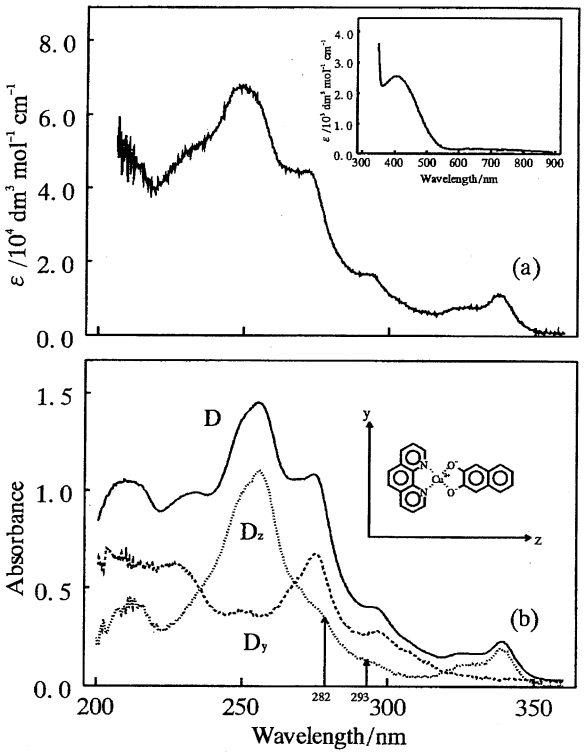

Fig. 6. The electronic absorption and reduced spectra of [Cu(ndo)(phen)]; (a) the absorption spectrum in methanol; (b) the reduced spectra in the PVA film.

and the y-axis polarized 308, 296, 275, and 251 nm ones to the $\pi\pi^*_3$, $\pi\pi^*_4$, $\pi\pi^*_9$, and $\pi\pi^*_{14}$ transitions, respectively (Table 4). The 255.5 nm band is due to an overlap of the $\pi\pi^*_{11}$ and $\pi\pi^*_{13}$ transitions, and the 229 nm band of the $\pi\pi^*_{16}$ and $\pi\pi^*_{17}$ transitions. The excited-state wavefunctions and MO's of [Cu(ndo)(phen)] are shown in Eq. 3 and Fig. 7, respectively.

$$\Psi_1 = 0.7773\,\chi_{13,17} - 0.6084\,\chi_{14,20} + \cdots$$
$$\Psi_2 = -0.5839\,\chi_{11,15} - 0.7569\,\chi_{12,16} + \cdots$$
$$\Psi_3 = 0.4967\,\chi_{11,16} - 0.8535\,\chi_{12,15} + \cdots$$
$$\Psi_4 = -0.9342\,\chi_{14,17} + \cdots$$
$$\Psi_5 = 0.5132\,\chi_{13,16} - 0.8355\,\chi_{14,15} + \cdots$$
$$\Psi_6 = -0.5812\,\chi_{13,15} + 0.7883\,\chi_{14,16} + \cdots$$
$$\Psi_7 = 0.8328\,\chi_{13,16} + 0.5263\,\chi_{14,15} + \cdots$$
$$\Psi_8 = 0.7883\,\chi_{13,15} + 0.5930\,\chi_{14,16} + \cdots$$
$$\Psi_9 = 0.6826\,\chi_{11,16} + 0.4515\,\chi_{12,15} + \cdots$$
$$\Psi_{10} = -0.6065\,\chi_{11,15} - 0.5891\,\chi_{12,16} + \cdots$$
$$\Psi_{11} = -0.5273\,\chi_{13,17} - 0.6665\,\chi_{14,20} + \cdots$$
$$\Psi_{12} = 0.3428\,\chi_{12,19} + 0.6481\,\chi_{13,20} + \cdots$$
$$\Psi_{13} = 0.5291\,\chi_{10,20} + 0.3391\,\chi_{12,18} + 0.6057\,\chi_{13,20} + \cdots \quad (3)$$
$$\Psi_{14} = -0.4074\,\chi_{11,16} - 0.5339\,\chi_{13,20} + \cdots$$
$$\Psi_{15} = 0.2615\,\chi_{8,16} + 0.4634\,\chi_{11,15} + 0.6896\,\chi_{12,18} - 0.2368\,\chi_{14,20} + \cdots$$
$$\Psi_{16} = 0.5427\,\chi_{10,17} - 0.5753\,\chi_{14,18} + \cdots$$
$$\Psi_{17} = 0.3922\,\chi_{10,17} + 0.7976\,\chi_{14,18} + \cdots$$
$$\Psi_{18} = -0.9746\,\chi_{13,18} + \cdots$$
$$\Psi_{19} = 0.7972\,\chi_{7,15} + 0.3842\,\chi_{8,16} + \cdots$$
$$\Psi_{20} = 0.6398\,\chi_{10,17} - 0.7580\,\chi_{14,22} + \cdots$$
$$\Psi_{21} = -0.5240\,\chi_{11,18} + 0.7921\,\chi_{12,19} + \cdots$$
$$\Psi_{22} = 0.4927\,\chi_{7,16} + 0.7761\,\chi_{8,15} + \cdots$$
$$\Psi_{23} = 0.9847\,\chi_{14,19} + \cdots$$
$$\Psi_{24} = 0.8547\,\chi_{13,19} + \cdots$$
$$\Psi_{25} = 0.9838\,\chi_{10,15} + \cdots$$
$$\Psi_{26} = 0.6244\,\chi_{8,16} + 0.3670\,\chi_{9,17} + 0.5202\,\chi_{11,19} + \cdots$$

To Ψ_1, $\chi_{13,17}$ and $\chi_{14,20}$ are contributed by 60 and 37%, respectively. Since the all MO's ϕ_{13}, ϕ_{14}, ϕ_{17}, and ϕ_{20} are localized on the ndo moiety, the observed 339.0 nm band

Table 4. Comparison of the Calculated and Observed Results for the Electronic Transitions of [Cu(ndo)(phen)]

		Transition energy (nm)		Intensity		Polarization direction	
		Calcd	Obsd[a]	Calcd[b]	Obsd[c]	Calcd	Obsd[a]
			650[d),e]		—		—
			400[d),f]		—		—
$\pi\pi^*_1$	($^1A_1$)	341.0	339.0	0.04402	0.186	z	z
$\pi\pi^*_2$	($^1A_1$)	337.2		0.00001		z	
$\pi\pi^*_3$	($^1B_1$)	308.7	308	0.11790	0.175	y	y
$\pi\pi^*_4$	($^1B_1$)	303.0	296	0.11611	0.270	y	y
$\pi\pi^*_5$	($^1A_1$)	297.6	293	0.00049	0.135	z	z
$\pi\pi^*_6$	($^1B_1$)	296.0		0.00000		y	
$\pi\pi^*_7$	($^1A_1$)	291.1	282	0.00016	0.382	z	z
$\pi\pi^*_8$	($^1B_1$)	290.3		0.00000		y	
$\pi\pi^*_9$	($^1B_1$)	281.3	275	0.74368	0.629	y	y
$\pi\pi^*_{10}$	($^1A_1$)	264.5	269	0.82390	0.494	z	z
$\pi\pi^*_{11}$	($^1A_1$)	247.5	255.5	1.37137	1.000	z	z
$\pi\pi^*_{12}$	($^1B_1$)	238.4		0.00458		y	
$\pi\pi^*_{13}$	($^1A_1$)	234.7	(255.5)	0.68062	(1.000)	z	(z)
$\pi\pi^*_{14}$	($^1B_1$)	234.2	251	1.46377	0.360	y	y
$\pi\pi^*_{15}$	($^1A_1$)	231.4	236	0.04165	0.517	z	z
$\pi\pi^*_{16}$	($^1B_1$)	229.1	229	0.17703	0.472	y	y
$\pi\pi^*_{17}$	($^1B_1$)	229.1		0.09592		y	
$\pi\pi^*_{18}$	($^1A_1$)	227.1		0.00013		z	
$\pi\pi^*_{19}$	($^1A_1$)	224.4		0.00339		z	
$\pi\pi^*_{20}$	($^1B_1$)	220.7		0.00174		y	
$\pi\pi^*_{21}$	($^1B_1$)	216.2		0.00084		y	
$\pi\pi^*_{22}$	($^1B_1$)	207.5		0.03180		y	
$\pi\pi^*_{23}$	($^1A_1$)	206.2		0.00002		z	
$\pi\pi^*_{24}$	($^1B_1$)	204.9		0.00001		y	
$\pi\pi^*_{25}$	($^1A_1$)	204.6		0.00000		z	
$\pi\pi^*_{26}$	($^1A_1$)	203.4	212	0.29054	0.416	z	z

a) Observed in the PVA matrix at room temperature. y: Perpendicular to the C_2 axis in the molecular plane. z: The C_2 axis. b) Oscillator strength. c) Relative intensities with respect to the 255.5 nm band. d) Observed in methanol. e) d–d Band. f) Intramolecular CT band between copper(II) and ndo.

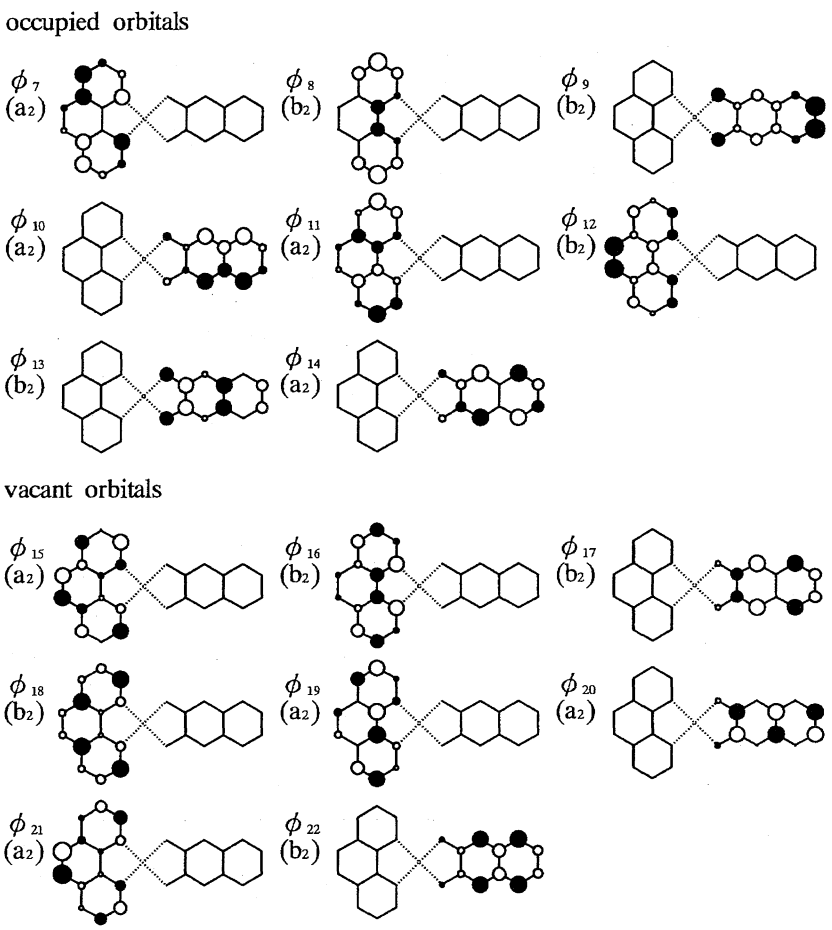

Fig. 7. Diagrammatic representations of SCF MO's of [Cu(ndo)(phen)].

can be regarded as being a localized electronic transition on ndo. Similarly, the 296 nm band is a localized transition on the ndo moiety. On the other hand, the observed 308 nm transition is localized on the phen moiety, because to Ψ_3 corresponding to this observed transition, $\chi_{11,16}$ and $\chi_{12,15}$ are contributed by 25 and 73%, respectively, in which MO's ϕ_{11}, ϕ_{12}, ϕ_{15}, and ϕ_{16} are due to the phen moiety. Similarly, the observed 275 and 269 nm transitions are localized on phen. As described above, the observed 255.5 nm band is due to an overlap of the $\pi\pi^*_{11}$ and $\pi\pi^*_{13}$ transitions. The $\pi\pi^*_{11}$ transition is localized on phen. The $\pi\pi^*_{13}$ transition is a superimposition of $\chi_{10,20}$, $\chi_{12,18}$, and $\chi_{13,20}$, in which $\chi_{12,18}$ is one electronic excitation configuration localized on phen, and $\chi_{10,20}$ and $\chi_{13,20}$ are on ndo, thus indicating that the two π-electronic systems almost localized on the two moieties phen and ndo can mix with each other through configuration interactions. Similarly, the 251, 236, and 212 nm bands arise through configuration interactions between the two locally excited configurations localized on phen and ndo. To Ψ_5 corresponding to the observed 293 nm transition, $\chi_{13,16}$ and $\chi_{14,15}$ are contributed by 26 and 70%, respectively. MO's ϕ_{13} (HOMO$-$1, b_2) and ϕ_{14} (HOMO, a_2) are localized on ndo, and ϕ_{15} (LUMO, a_2) and ϕ_{16} (LUMO+1, b_2) are localized on phen. Thus, the observed 293 nm band can be regarded as being due to an LL′CT transition from ndo to phen. From a similar consideration, the observed 282 nm band can be assigned as an LL′CT transition from ndo to phen. The above results indicate that the π-electronic systems localized on ndo and phen can interact significantly with each other. It is also found that the observed 229 nm transition is a mixture of a localized transition on ndo and an LL′CT transition from ndo to phen.

This work was partly supported by Grants-in-Aid for Scientific Research Nos. 07804041, 08554026, and 07454173 from the Ministry of Education, Science, and Culture. Financial support from the Yamada Research Fund from Yamada Science Foundation is greatfully acknowledged.

References

1) H. Sigel, *Angew. Chem., Int. Ed. Engl.*, **14**, 394 (1975).
2) I. P. Mavani, C. R. Jejurkar, and P. K. Bhattacharya, *J. Indian Chem. Soc.*, **49**, 469 (1972).
3) I. M. Procter, B. J. Hathaway, and P. G. Hodgson, *J. Inorg. Nucl. Chem.*, **34**, 3689 (1972).
4) Y. Yamada, T. Hoshi, and Y. Fukuda, *J. Coord. Chem.*, **38**, 1 (1996).
5) Y. Yamada, Y. Fukuda, and T. Hoshi, *Mol. Cryst. Liq. Cryst.*, **286**, 23 (1996).
6) D. G. Brown, J. T. Reinprecht, and G. C. Vogel, *Inorg. Nucl. Chem. Lett.*, **12**, 399 (1976).
7) T. Hoshi, Y. Inomaki, M. Wada, Y. Yamada, J. Okubo, M.

Kobayashi, and H. Inoue, *Ber. Bunsenges. Phys. Chem.*, **98**, 585 (1994).

8) F. A. Walkeer, H. Sigel, and D. B. McCormick, *Inorg. Chem.*, **11**, 2756 (1972).

9) T. Hoshi and Y. Tanizaki, *Z. Phys. Chem., Neue Folge*, **71**, 230 (1970).

10) T. Hoshi, T. Kawashima, J. Okubo, M. Yamamoto, and H. Inoue, *J. Chem. Soc., Perkin Trans. 2*, **1986**, 1147.

11) H. Inoue, T. Hoshi, T. Masamoto, J. Shiraishi, and Y. Tanizaki, *Ber. Bunsenges. Phys. Chem.*, **75**, 441 (1971).

12) T. Hoshi, J. Yoshino, and K. Hayashi, *Z. Phys. Chem.*, **83**, 31 (1973).

13) C. G. Pierpoint and R. M. Buchanan, *Coord. Chem. Rev.*, **38**, 45 (1981).

14) W. Fitzgerald, J. Fooley, D. McSweeney, N. Ray, D. Sheanon, S. Tyagi, B. Hathaway, and P. O'Brien, *J. Chem. Soc., Dalton Trans.*, **1982**, 1117.

15) M. Julve, J. Faus, M. Verdauguer, and A. Gleizes, *J. Am. Chem. Soc.*, **106**, 8306 (1984).

16) A. Fabretti, G. Franchini, P. Zannini, and M. Divaira, *Inorg. Chim. Acta*, **105**, 187 (1985).

17) I. Castro, J. Faus, M. Julve, M. C. Munoz, W. Diaz, and X. Solands, *Inorg. Chim. Acta*, **179**, 59 (1991).

18) T. Fujii and S. Suzuki, *Bull. Chem. Soc. Jpn.*, **49**, 2892 (1976).